PROCEEDINGS OF SCIENCE

LA-UR-15-22439

The Set of Diagnostics for the First Operation Campaign of the Wendelstein 7-X Stellarator

Ralf König*,[1]
E-mail: Ralf.Koenig@ipp.mpg.de

J. Baldzuhn[1], W. Biel[2], C. Biedermann[1], H. S. Bosch[1], S. Bozhenkov[1], B. Brotas de Carvalho[3], R. Burhenn[1], B. Buttenschön[1], G. Cseh[4], A. Czarnecka[5], M. Endler[1], V. Erckmann[1], T. Estrada[6], J. Geiger[1], O. Grulke[1], D. Hartmann[1], D. Hathiramani[1], M.Hirsch[1], S. Jabłonski[5], M. Jakubowski[1], J. Kaczmarczyk[5], T. Klinger[1], S. Klose[1], G. Kocsis[4], P. Kornejew[1], A. Krämer-Flecken[2], T. Kremeyer[7], M. Krychowiak[1], M. Kubkowska[5] , A. Langenberg[1], H. P. Laqua[1], M. Laux[1], Y. Liang[2], A. Lorenz[1], A., O. Marchuk[2], V. Moncada[8], O. Neubauer[2], U. Neuner[1], J. W. Oosterbeek[9], M. Otte[1], N. Pablant[10], E. Pasch[1], T. S. Pedersen[1], K. Rahbarnia[1], L. Ryc[5], O. Schmitz[7], W. Schneider[1], H. Schuhmacher[11], B. Schweer[2], T. Stange[1], H. Thomsen[1], J.-M. Travere[8], T. Szepesi[4], U. Wenzel[1], A. Werner[1], B. Wiegel[11], T. Windisch[1], R. Wolf[1], G. A. Wurden[12], D. Zhang[1], A. Zimbal[11], S. Zoletnik[4] and the W7-X Team

[1]*Max Planck Inst. for Plasma Physics,17491 Greifswald, Germany,*
[2]*Institute of Energy- and Climate Research, Forschungszentrum Jülich GmbH, D-52425 Jülich, Germany*
[3]*Instituto de Plasmas e Fusao Nuclear Instituto Superior Tecnico, Lisbon, Portugal*
[4]*Wigner RCP,RMI, Konkoly Thege 219-33, H-1121, Budapest Hungary;*
[5]*IFPiLM, Hery Street 23, 01-497 Warsaw, Poland*
[6]*Laboratorio Nacional de Fusi´on, CIEMAT, Avenida Complutense, Madrid, Spain*
[7]*Univ. of Wisconsin, Dept. of Engineering Physics, 1500 Engineering Drive, Madison, WI 53706*
[8]*CEA, IRFM, F-13108 Saint-Paul-lez-Durance, France*
[9]*Technical University of Eindhoven, Eindhoven, The Netherlands*
[10]*Princeton Plasma Physics Laboratory, Princeton, New Jersey 08543, USA*
[11]*Physikalisch-Technische Bundesanstalt, Bundesallee 100, 38116 Braunschweig, Germany*
[12]*Los Alamos National Laboratory, Los Alamos, NM 87544, USA*

ABSTRACT: Wendelstein 7-X (W7-X) is a large optimized stellarator (B=2.5T, V=30m^3) aiming at demonstrating the reactor relevance of the optimized stellarators. In summer this year (2015) W7-X will begin its first operation phase (OP1.1) with five inertially cooled inboard limiters made of graphite. Assuming the heat loads can be spread out evenly between the limiters, 1 second discharges at 2 MW of heating power could be run in OP1.1. The expected plasma parameters will be sufficient to demonstrate the readiness of the installed diagnostics and even to run a first physics program, albeit restricted to relatively short pulses, and limiter configurations. The diagnostics available for this first operation phase, including some special limiter diagnostics, and their capabilities are being presented.

First EPS Conference on Plasma Diagnostics - 1st ECPD
14-17 April 2015,
Villa Mondragone , Frascati (Rome) Italy

*Speaker

1. Introduction

The Wendelstein 7-X (W7-X) stellarator[1,2,3] with its superconducting coil system will be taken towards one of its central aims of demonstrating quasi-continuous plasma operation in three steps. For the upcoming very first plasma operation phase OP1.1 five inertially cooled inboard limiters made of graphite have been installed. These will, in the run-up to OP1.2, which starts one year later, be exchanged by 10 inertially cooled test divertor units (TDU). The shape of the TDU exactly mimics the actively cooled high heat flux (HHF) divertor, which will finally be available for pushing to quasi-continuous operation with the beginning of OP2, currently foreseen to start in 2019. With very few exceptions, all installed diagnostics are already prepared for this later, highly demanding, high heating power (P_{ECRH}~10 MW), quasi-continuous operation phase.[4,5,6]

The presently ongoing commissioning of W7-X has started about a year ago with the closure of the cryostat. The installation of the in-vessel components has been completed by the end of last year. At the beginning of March this year the plasma vessel leak testing of the plasma vessel has started and the cool down to less than 4 K been successfully demonstrated, so that the commissioning of the magnet system can now begin in early May. This demonstrates that starting the first plasma operation period of 13 weeks duration in late summer this year seems realistic. The main aim of OP1.1 is to enable an early commissioning and demonstration of the safe system operation of the main W7-X device systems, like vacuum, vessel conditioning (baking, helium glow discharge cleaning), cryogenics, magnetic field coils and the ECRH heating. Of course this phase will also be used for commissioning and testing of most of the diagnostics required for OP1.2, albeit many of them being not yet fully integrated into the standard W7-X data acquisition and control system at this stage.

The brief first campaign OP1.1 will also be used to perform some very first physics experiments.[7] With the carbon tiles not yet attached to the heat shields and the already installed divertor frame being unprotected, particular care has been taken in designing a limiter magnetic configuration which ensures that these components are not exposed to any convective loads. With the limiters being simply attached to the heat shield structures we expect to be able to run 1 second discharges at 2 MW of heating power (ECRH), assuming the heat loads can be spread out evenly across the limiters. The plasma parameters expected to be achievable under these conditions ($T_e < 3.5$keV, $T_i < 0.9$keV, $n_e < 2\ 10^{19} m^{-3}$) are expected to be sufficient to demonstrate the readiness of the installed diagnostics and even to run a small first physics program, initially with helium and possibly even a few weeks with hydrogen.

2. Diagnostic for OP1.1

Fig. 1 shows for one of the 5 modules of W7-X the location of the port types available for diagnostics. In the other modules the port locations are mostly identical, only few ports have a slightly different shape and orientation.

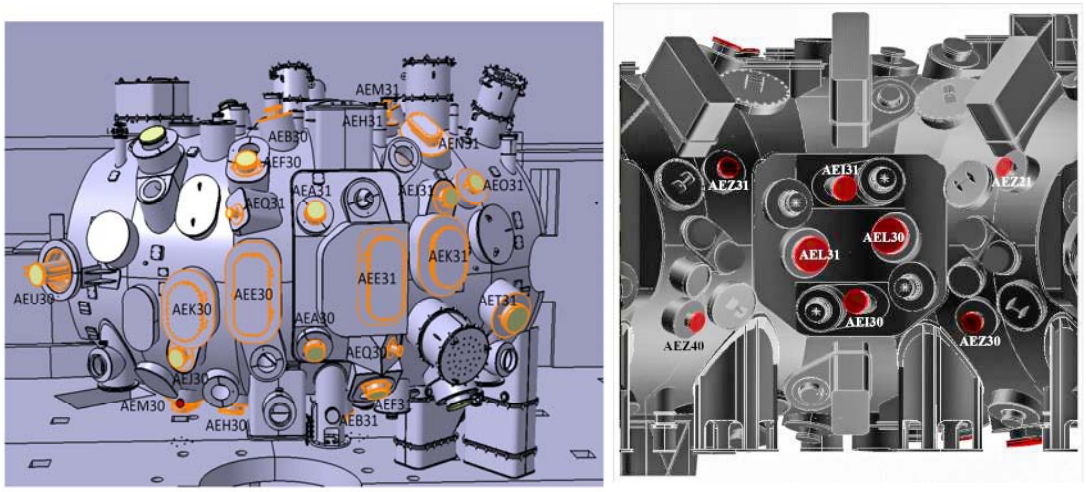

Fig. 1: Diagnostics ports in half modules 30 & 31:
left figure outer view, right figure view from torus centre.

2.1. Core plasma diagnostics

2.1.1 Neutron counters

Three neutron counter systems[8,9] have been installed on W7-X, one sitting about 3.9 m above the centre of the torus at R=0 m, while the two others are mounted on top of the cryostat vessel viewing the plasma in half modules 10 and 30. The central system consists of 5 counter tubes of different sensitivity to thermal neutrons, whereas the two peripheral ones contain 4 counter tubes, inserted in a specially designed moderator. The detectors have different sensitivities in order to allow measurement of the neutron yield of the plasma over more than five orders of magnitude with <15% statistical uncertainty in time intervals of 5 ms. The design aims of the neutron monitors were confirmed by investigations in the reference radiation fields at the Physikalisch-Technische Bundesanstalt, Braunschweig, Germany, in 2014. In January 2015 they were calibrated at W7-X, using an in-vessel railway to transport a ^{241}Am/Be calibration source along the midplane of the plasma vessel. A relative standard uncertainty of <3% has been achieved for the calibration factors, i.e. the ratio of the neutrons starting from the calibration source and the number of counts observed with the monitors.

2.1.2 Flux surface measurements

Three flux surface measurement systems have been built, of which two have been installed in HM10 and HM30 for OP1.1. Each system consists of a scintillator coated rod with an electron gun at its tip. The specially designed drive allows full coverage of the roughly triangular shaped plasma vessel cross section and pulling back of the system behind an actively coolable shutter during plasma operation. For the observation of the fluorescent emission generated at the spot where the electron beam hits the rod, two PCO PixelFly cameras installed inside the AEQ21 and AEQ51 ports are being used. A spatial resolution of 2 mm will be achievable. As spatial reference, 4 metal-coated optical fibres were integrated into the wall structures in each plane, which are being illuminated from the outside of the plasma vessel. The measurements will start in May, i.e. right from the beginning of the commissioning of the superconducting coils, in order to learn how to correct any residual error fields with the trim

coils and gather information how to correct for the effects resulting from the deformation of the coils with increasing field strengths.[3]

2.1.3 Equilibrium magnetics and Mirnov coils

The major part of the magnetic diagnostics, consisting of 3 diamagnetic loops, 3 continuous and 5 segmented Rogowski coils, 40 saddle coils and 125 Mirnov coils, have been fully installed and will be available in OP1.1.[10] The diamagnetic loops are designed to resolve the plasma energy with an accuracy of 10 kJ (where the expected maximum value is ~5 MJ) and a time resolution of better than 1 ms. The Rogowski coils are designed to measure the total toroidal plasma current with an accuracy of 100 A (where maximum net toroidal currents of ~200 kA are predicted in certain discharge scenarios for the sum of bootstrap currents and microwave or neutral beam driven currents). The saddle coils and the segmented Rogowski coils deliver information to determine the poloidal and radial distribution of the toroidal current density (e. g., Pfirsch-Schlüter currents) in the framework of an equilibrium reconstruction. The Mirnov coils are arranged in three complete and one partial poloidal array with up to 41 coils in one array and will serve to resolve the poloidal mode structure of magnetic fluctuations, e.g., due to MHD modes. The low self-inductance, short signal cables, and their location behind gaps between the wall protection tiles will allow observing frequencies up to ~1 MHz.

The design of all the installed magnetic diagnostics with their in-vessel signal cables is already suitable for long-pulse discharges, taking into account microwave stray radiation and further thermal loads from the back faces of wall protection elements, and the electronics and data acquisition modules are a special development for the numerical integration during discharges of up to 30 min.[11]

2.1.4 Single channel dispersion interferometer

The line of sight averaged electron density will be provided by a single channel dispersion interferometer[12,13] equipped with a Field Programmable Gate Array (FPGA) based data analysis. In OP1.1 we aim at demonstrating the real time capabilities of the W7-X dispersion interferometer set-up,[14,15] but without the gas feedback loop yet being implemented. The time resolution for the line of sight integrated density measurements is 20 μs. The lower limit of the density measurements of about 3 10^{17}m^{-2} to ~1 10^{18} m^{-2} is determined by the noise level and a gradual drift caused by air temperature and humidity induced dispersion variations, while at the upper end the first fringe jump will occur at 1.4 10^{20} m^{-2}. The accuracy of the density measurements is about ±3 10^{17}m^{-2}. With the CO_2 (10.6 μm) and the frequency doubled laser beam (5.3 μm) line running collinear with the laser beam of the Thomson scattering diagnostic through the shared ports AET30, AEZ30 and the plasma centre, the line of sight averaged densities measured by the interferometer can also be directly used for cross calibration with the Thomson Scattering diagnostic.

2.1.5 Thomson Scattering

The ~ 5-7 mm diameter beams of the two Nd-YAG lasers (repetition freq. 10Hz at 4J, 20Hz at 2J, 2J/pulse, 10ns pulse duration) pass through the ports AET31, AEZ31 and the plasma centre. The scattered light is being observed from the AEM31 (outer half profile) and the

AEN31 (inner half profile) ports.[4] In OP1.1 the observation optics in the AEM31 port is equipped only with ten optical fibres of two different lengths, providing a spatial resolution of 2 cm at the plasma centre and 3 cm at the edge, over the outer half profile. By making use of the time delay between the different fibre lengths, two fibres can be fitted to each of the five polychromators. The polychromators consist of 1 Raman filter for calibration and 4 suitably selected filters to cover the temperature range from 20 eV to 10 keV and the density range from 5 10^{18} m^{-3} to 5 10^{20} m^{-3}, both with an accuracy of ~5%. The data acquisition system has a dynamic range of 12 bit and a time resolution of 1ns.

2.1.6 Electron cyclotron emission (ECE) diagnostic

The electron temperature will be measured by a 32 channel Electron Cyclotron Emission (ECE) diagnostic applying a heterodyne radiometer followed by a filter bank.[15] A slim Gaussian beam characteristics with radius w_0=20mm at its waist in the plasma centre, minimizes the emitting volume for each frequency interval, thereby maximizing the radial resolution. The filter bandwidth has been adapted to the optical depth of the corresponding emitting layers resulting in a radial resolution of 1 to 3cm. An additional 16 channel zoom system selects a 4 GHz wide part of the spectrum at suitable radii using a tuneable second local oscillator. This span corresponds to a radial range of Δr=6cm at the high-field side or ~15cm at the low-field side. The zoom device is particularly dedicated to measuring the power deposition profile via heat wave analysis around the radius of the ECRH heating and to ELM studies. For in-situ calibration at any time the ECE system includes a complete copy of the in-vessel system just outside the cryostat in air, which can be switched to.

The above system is complemented by an additional small horn antenna, which is integrated into the heat shield, providing a view along the same line of sight from the high-field side, thereby allowing to also measure the emission from supra-thermal and current driven electrons.[15]

2.1.7 Electron cyclotron absorption (ECA) and stray radiation diagnostic

Especially in OP1.1, with starting W7-X for the very first time, initially relatively high impurity influx levels need to be expected and may lead to increasing strong energy losses and thereby decreasing electron temperatures in the course of a discharge, which could result in early discharge termination. To provide a means for an early detection of the transition towards such a scenario, the ECRH wall protection tiles opposite to the ECRH ports in module 1 and 5 (AEA11, AEE10, AEA51, AEE51) have been equipped with 2 x 63 open waveguide antennas. Each of them picks up a small part of the ECRH beam reaching the corresponding tiles and allows measuring the amplitude, polarization and position of the beam. Besides the determination of the power absorbed in the plasma, the electron cyclotron absorption (ECA) diagnostic can provide, for selected cases, the optical depth for the EC radiation at different radial positions, necessary for correcting the electron temperatures determined by the ECE diagnostic for optically 'grey' plasmas ($T_e < 0.5$ keV, $n_e < 2 \cdot 10^{19}$ m^{-3}).
Furthermore, an ECRH stray radiation monitor, consisting of an oversized waveguide with a broad antenna characteristic, combined with a detection optics and a propylene diffuser in front of the detector, has been installed in each of the 5 vessel modules, to provide an interlock signal for the ECRH system, in case of unacceptably low plasma absorption. In addition, each of the 4

ECRH launchers is equipped with a NIR camera described in section 2.2.2. They should detect arcing on the protection tiles and thermal overloading in the long pulse discharges in OP2.

2.1.8 Reflectometer systems

Two reflectometer systems[15] are installed in port AEA21. The V-band hopping Doppler reflectometer (50-70 GHz), provided by CIEMAT,[16] is designed to resolve density fluctuations in the steep edge gradient region around r/a=0.85-0.95 (~2.5 cm) with a fixed incidence angle (18°), which translates into a selected fluctuation wavelength of ~ 1cm. The Ka-band poloidal correlation hopping reflectometer (25-50 GHz), provided by Forschungszentrum Jülich (FZJ), consists of an array of one launching and four receiving antennae,[17] which observe density fluctuations around the separatrix (r/a~0.95-1) sampled at 4 MHz. From the multiple antennae setup, parameters like propagation velocities, correlation lengths, and the local magnetic field pitch angle can be derived. The radial resolution is in the range of a few millimetres, depending on the amplitude of the density fluctuations.

2.1.9 High resolution X-ray imaging system (HR-XIS)

The high resolution X-ray imaging system has been set up by FZJ.[18] The diagnostic provides line integrated measurements of standard plasma parameters like ion and electron temperatures, plasma rotation and argon impurity densities. Therefore, helium-like states of argon are monitored along one central and one line of sight across the lower half of the flux surfaces in a poloidal plane, using two CCD cameras and optional a gas detector. Wavelength selection by Bragg-reflection (λ = 4 Å) is achieved with a spherically bent crystal, yielding an ion and electron temperature resolution of 90 eV, with an electron temperature range between 0.3 to 4 keV. As an upgrade, the spectrometer allows to install up to 6 spherically bent crystals on a rotatable mount, giving access also to the highest ionization states of several other impurity species like e.g. iron or sulfor.[19]

2.1.10 X-ray imaging crystal spectrometer (XICS)

The X-ray imaging crystal spectrometer[19] is being provided by PPPL, Princeton, USA. The XICS diagnostic will provide profiles of the ion-temperature T_i, electron-temperature T_e, poloidal flow velocity v_p and impurity ion density for the Ar^{16+} charge state.[20] Tomographic inversion, using a known plasma equilibrium, is used to infer the local plasma parameters from the line integrated data.[21] This system will have a maximum time resolution of 5ms, a spatial resolution of approximately 2cm, and spatial coverage from the core to a normalized minor radius of $\rho \approx 0.82$. The diagnostic will be installed at the AEK31 port, which is a large radially viewing midplane port. A spherical quartz crystal, with a cut along the (1,1,0) axis, will be used to provide dispersion and imaging of the plasma generated x-rays. For x-ray detection, the system will utilize a water cooled Pilatus 300K-W hybrid-pixel CMOS detector from Dectris Ltd.. The system is expected to measure T_e with a resolution of 20eV, T_i with a resolution of 20eV and v_p with a resolution of 5 km/s. To obtain sufficient signal for these measurements, an argon density of approximately $n_{Ar}/n_e = 10^{-5}$ is required. Argon puffing will be achieved through the W7-X gas injection system or through the helium beam diagnostic system.

2.1.11 Pulse Height Analysis System (PHA)

The PHA system has been developed and manufactured at IPPLM, Warsaw,[22] while support and infrastructure has been provided by IPP. Three silicon drift detectors equipped with different absorber foils are mounted in a vacuum chamber behind a set of 3 remotely controlled exchangeable filters with Be-foil thicknesses varying between 0 and 500µm to record a wide range of x-ray energies with optimized resolution. An adaptable entrance aperture consisting of two crossed piezo-slits (max. width: 1.35 mm) allows to minimize degradation of the detector resolution at high intensities and optimal throughput at low intensity. This line of sight system with three different energy bandwidths is installed at port AEK50 and allows to determine Z_{eff}, measure various impurity species, the central electron temperature and investigate supra-thermal tails in the spectra over a cross section of ~10x10 cm^2 with a time resolution of 100ms, covering the energy range from 250eV up to 20keV with a resolution not worse than 200 eV (nominally 130 eV@5.9 keV).[23] For in-situ calibration a mini X-ray tube has been integrated in the system which illuminates the stainless steel plate also containing Cu and Ti, thereby inducing a fluorescent signal, suitable for calibration over the large energy range. For data acquisition a 4-channel digital X-ray processor, Mercury-4, from XIA LLC is being used.

2.1.12 High Efficiency eXtreme ultraviolet Overview Spectrometer (HEXOS)

The HEXOS survey spectrometer system[24,25,19] consists of 4 VUV spectrometers with different incidence angles, ranging from near normal incidence (45 deg.) to grazing incidence (86 deg.). Two sets of two spectrometers are mounted in single frames back to back, in total covering the spectral range from 2.5 to 160 nm. The system has been provided by FZJ and has already been calibrated[26] and extensively tested on TEXTOR together with a W7-X Mini-CoDaC control and data acquisition system. The HEXOS device, which is installed in the plasma vessel midplane at the AEU10 port, will provide detailed spectral information in particular on the medium- and high-Z impurities. Each instrument is equipped with a linear diode array (1024 pixels) with an attached multi-channel plate image intensifier.[27] The time resolution of the detectors is 1 ms.

2.1.13 Horizontal and vertical bolometer systems

A horizontal and a vertical bolometer system,[28] equipped with 32 and 40 channels, respectively, has been installed in the AEU30 and AEV21 ports, allowing tomographic reconstruction of the 2D emission profiles in the triangular shaped plane of W7-X. A spatial resolution of about 5 cm and a time resolution of 3 ms are expected for OP1.1. Additionally, on the secondary detector arrays of the two bolometer systems 8 channels, each covered with 10µm-Be filter, are available for measuring the soft X-ray (>800eV) emission from the plasma centre.

2.1.14 Z_{eff} Bremsstrahlung measurements

In OP1.1 only a single line of sight Z_{eff} bremsstrahlung system is installed, looking radially through the plasma centre via optical windows in the port lids of the oppositely located ports AET40 and AEZ40. The light is being collected by a camera lens and then transported via a 1mm diameter optical fibre to a micro-spectrometer in the lab, covering the spectral range from 350 to 1000 nm with a time resolution of 5 ms. A Bayesian analysis procedure, in which the

spectral lines are treated as nuisance parameters, will be used to derive Z_{eff} from the underlying background over the entire spectral range.[29]

2.2 Edge and limiter plasma diagnostics

2.2.1 Video diagnostic

Ten video diagnostics systems[31] developed and provided by the Wigner Institute, Budapest, have been installed in all 10 AEQ ports, providing a toroidal view of the plasma and the entire plasma vessel wall. The price to pay to gain a toroidal view of the plasma is that the 10 cm diameter port bends around a coil. Therefore the EDICAM[31,32] CMOS camera with its lens needs to be transported through the port, until it locks to a ring welded into the port close to the plasma vessel opening. This made it necessary to mount the vacuum window from the in-vessel side to the same welded ring inside the port. IPP has provided the diagnostics front end consisting of the window, a small uncooled shutter and a water cooled plasma facing front plate with a pinhole, which also forms the entrance pupil of the optics. The 1280x1024 pixel cameras provide a spatial resolution of 2 mm at all distances and a time resolution of 2.5 ms in full frame mode. The highly sophisticated features of the EDICAM system, of e.g. non-destructive and independent region-of-interest read-out possibilities, will not be made use of in OP1.1. The simultaneous control and display of all cameras in the control room will be provided by the VIDACS[30] program developed by the Wigner Institute.

Two of the ten systems (at the AEQ21 and AEQ51 ports) are in OP1.1 equipped with PCO PixelFly CCD cameras to allow a higher sensitivity of the flux surface measurements. To further improve the signal quality for these measurements, also a higher throughput lens is being used and at one port the water cooled pinhole plate has not yet installed for this reason. At port AEQ30 a damaged bellow made it necessary to evacuate the entire port tube. To maintain the observation from this port, a fibre optic image guide with 800x1000 pixels and an optic has been installed, instead of the EDICAM capsule, in the port bellow, to transport the light to the outside of the port where in parallel with the EDICAM a fast camera (Phantom from PPPL Princeton and/or Photron SA5 from Wigner Institute) will be installed.

2.2.2 2D NIR/visible limiter observation

10 immersion tube based systems with three observation windows at their plasma facing end and a rotating shutter blade in front are installed at the 10 AEF ports for later divertor observation in OP1.2.[33] In the first campaign these systems will also provide a reasonable view of the 5 limiter tiles. Directly behind the windows 2 magnetic field compatible visible light cameras and one near infrared (NIR) camera are installed. The cameras are equipped with wide angle viewing optics, having a field of view of 86° or 136° and some with interference filters for H_α, CII, CIII radiation. The visible cameras (Raptor Photonics: CYGNET 2048x2048 pixels) and the NIR cameras (SONY XC-EI50CE: 768 x 494 pxl.), both have a time resolution of 40ms.

An additional immersion tube, equipped with the same NIR camera, has been integrated into each of the four ECRH launchers to monitor the temperature of the ECRH wall protection tiles and also the temperature distribution patterns on the limiters opposite to the launchers in

modules 1 and 5. For the NIR cameras CEA has provided the software for camera control, data acquisition and storage of the data in the central data base.

Furthermore, port AEA30 has been equipped with a 216 mm diameter sapphire window for OP1.1, to allow high resolution nearly perpendicular observation of the central part of the limiter with a magnetically shielded, cooled 3-5 µm InSb IR camera (FLIR SC8303HD, 1344x768 pixels, 120 Hz frame rate, with a 200 mm f/4 lens) and a CMOS colour camera (Allied Vision Technologies Prosilica GX 1050 1024 x 1024 pixel, frame rate: 112 Hz) providing a spatial resolution of < 1 mm on the limiter surface.

2.2.3 Limiter integrated Langmuir probe arrays

In the 3rd tile from the top and bottom of the limiter in module 5 twenty Langmuir probe tips have been integrated, each, which will provide information on T_e, n_e, floating potential and the width of the heat deposition region. The Langmuir probes are cylindrical graphite tips with a diameter of 0.9 mm. The tips at the rim of the limiter are flush mounted, the other tips stick out of the limiter surface by about 1 mm. To measure the I/U-characteristics the bias-voltage can be swept between +/-200 V within a few milliseconds.

2.2.4 Neutral gas pressure measurements

Two ASDEX type neutral pressure gauges[34] have been installed in the midplane ports AEE30 and AEE50. These hot-cathode ionisation gauges were specially designed for operation in strong magnetic fields, operation in noisy environments and are well shielded from the plasma. To shield the interior of the pressure gauges from ECRH stray radiation and to ensure a gas exchange time constant of 1 ms, the screening box is perforated by a large number of 0.7 mm dia. holes, providing in total an open area equivalent to a 5.6 mm dia. hole. The position and orientation of the manometers has been carefully selected to ensure that magnetic configuration changes and in particular also operation of the trim coils do not affect the measurements. From the measured neutral flux densities pressures in the range from ~0.1 mbar up to 10^{-6} mbar can be derived.

In addition a Penning gauge developed at the University of Madison, Wisconsin, has been installed at AEE41, which will allow to also measuring the total neutral pressure and the partial pressures from spectroscopic analysis of the Penning discharge plasma. The system is quite comparable to the setup at TEXTOR[35] and LHD but is being improved towards higher sensitivity for the spectroscopic measurements. The main task of the system is to determine the helium partial pressure but other fractional neutral pressures of residual impurities like argon or nitrogen will be accessible too. With helium being the main working gas in OP1.1, this campaign is ideally suited to gain first experience with this diagnostic. Also, the system will aid quantitative characterization of the wall conditioning procedure.

2.2.5 Multi-purpose manipulator

The multi-purpose manipulator[36] developed at the research centre in Jülich, Germany, is installed at the AEK40 mid-plane port. The fast reciprocating head will be equipped with Langmuir probes, magnetic sensors and a piezo-controlled impurity gas inlet. Exposition of material samples for plasma wall interaction research is foreseen as well. This system will in OP1.2 allow to probe in the standard iota = 1 configuration the flux tube which connects the two divertor thermal He-beams. Already in OP1.1 investigation of the edge topology is envisaged.

2.2.6 Thermal He (Ne) diagnostic neutral beam and observation systems

The divertor thermal He-beam[37] gas boxes with 5 nozzles have been fitted through the AEH30 and AEH51 ports and for OP1.1, fixed to the divertor frames, while in OP1.2 they will be integrated into the divertor.[38] With the divertor observation endoscopes being under development for OP1.2 at the research centre in Jülich, in OP1.1 a simplified observation system has been installed, consisting of a bundle of 10 optical fibres fitted to a photo lens mounted directly behind a window installed in the AEI51 port lid and the same set-up with a single fibre at AEI30, mainly for first tests with Neon.[38] This will allow gaining some first experience with the operation of the beams and the signal analysis. An accompanying effort at UW Madison targets on improving the atomic physics data set in particular towards high density, low temperature divertor conditions and initial attempts for validation are considered for OP1.1.

Acknowledgments

This work has been carried out within the framework of the EUROfusion Consortium and has received funding from the Euratom research and training programme 2014-2018 under grant agreement No 633053. The views and opinions expressed herein do not necessarily reflect those of the European Commission.

References

[1] T. Klinger et al, Fus. Eng. Design **88**, 461 (2013)

[2] H. S. Bosch, et al., *Nucl. Fusion* **53** 126001 (2013) http://dx.doi.org/10.1088/0029-5515/53/12/126001

[3] S. Bosch, et al., IEEE Transactions on Plasma Science **42**, 432 (2014)

[4] R. König et al., Rev. Sci. Instrum. **81**, 10E133 (2010), http://dx.doi.org/10.1063/1.3483210

[5] R. König et al., Rev. Sci. Instrum. **83**, 10D730 (2012), http://dx.doi.org/10.1063/1.4733531

[6] R. König et al., Rev. Sci. Instrum. **85**, 11D818 (2014), http://dx.doi.org/10.1063/1.4889905

[7] T. S. Pedersen, Stellarator News 145, p. 1, 2014), http://web.ornl.gov/sci/fed/stelnews/pdf/sn145.pdf

[8] W Schneider et al, JINST **7**, C03025 (2012)

[9] B. Wiegel et al., Radiat. Prot. Dosimetry, **161** (1-4), 326 (2014)

[10] M. Endler et al., "Engineering Design for the Magnetic Diagnostics of Wendelstein 7-X", to be published

[11] A. Werner, et al., Rev. Sci. Instrum. **77** 10E307 (2006)

[12] Bagryanski P. A., *et al., Rev. Sci. Instrum.* **77**, 053501 (2006)

[13] T. Akiyama et al., *Development of a dispersion interferometer for magnetic confinement plasma and its application to high-pressure plasmas*, this conference

[14] P. Kornejew, et al., *Density Measurements at Fusion Experiments: 2-Color versus Dispersion Interferometer*, to be published

[15] M. Hirsch, et al., *Microwave and Interferometer Diagnostics prepared for first Plasma Operation of WENDELSTEIN 7-X*, this conference

[16] T. Happel, T. Estrada, E. Blanco, V. Tribaldos, A. Cappa, and A. Bustos, Rev. Sci. Instrum. **80**, 073502 (2009)

[17] A. Kraemer-Flecken et al., Rev. Sci. Instrum. **81**, 113502 (2010); http://dx.doi.org/10.1063/1.3497305

[18] G. Bertschinger, W. Biel, H. Jaegers et al. Rev. Sci. Instrum. **75**, 3727 (2004), http://dx.doi.org/10.1063/1.1781755

[19] H. Thomsen, *Startup impurity diagnostics in Wendelstein 7-X stellarator foreseen in the first operational phase,* this conference

[20] N. Pablant et al, Europhysics Conference Abstracts, Vol **38F**, p. P1.076 (2014). 41st EPS Conference on Plasma Physics.

[21] N. Pablant. et al., Review of Scientific Instruments, Vol **85**, p. 11E424 (2014)

[22] M. Kubowska,et al., *Laboratory tests of the Pulse Height Analysis system for Wendelstein 7-X*, this conference

[23] S. Jabłonski, et al., *Simulation of PHA Soft X-Ray Spectra Expected from W7-X*, this conference

[24] W. Biel et al., Rev. Sci. Instrum. **75**, 3268 (2004)

[25] W. Biel, et al., Rev. Sci. Instrum. **77**, 10F305 (2006)

[26] A. Greiche et al, Rev. Sci. Instrum. **79**, 093504 (2008)

[27] W. Biel et al, Rev. Sci. Instrum. **75**, 2471 (2004)

[28] D. Zhang et al., Rev. Sci. Instrum. **81,** 134 (2010)

[29] M. Krychowiak, et al, J. Appl. Phys. **96** , 4784 (2004); http://dx.doi.org/10.1063/1.1787135

[30] G. Koscis et al., Fus. Eng. Design, accepted for publication

[31] S. Zoletnik, et el., Fus. Eng. Design **88**, 1405 (2013)

[32] A. Szappanos et al. Fus. Eng. Design 85, 370. (2010)

[33] C. Biedermann, R. König, M. Jakubowski, D. Pilopp, T. Sunn Pedersen, *Visual and infrared imaging diagnostics at Wendelstein 7-X stellarator in the first operational phase*, this conference

[34] G. Haas, H.-S. Bosch, *In Vessel Pressure Measurement in Nuclear Fusion Experiments with ASDEX Gauges*, Vacuum **51**, 39 (1998)

[35] T. Denner, K.H. Finken and G. Mank, *Helium partial pressure measurement in a deuterium environment*, Rev. Science Inst. **67**, 3515-3520 (1996)

[36] O. Neubauer et al., *Diagnostic setup for investigation of plasma wall interactions at Wendelstein 7-X*, Fusion Engineering and Design (2015)

[37] O. Schmitz, et al., *Status of electron temperature and density measurement with beam emission spectroscopy on thermal helium at TEXTOR*, Plasma Phys. Control. Fusion **50**, 115004 (2008)

[38] M. Krychowiak, et al., Plasma Phys. Control. Fusion **53**, 035019 (2011), http://dx.doi.org/10.1088/0741-3335/53/3/035019